Biophysical Chemistry 41 (1991) 277–287
Elsevier Science Publishers B.V., Amsterdam

BIOCHE 01595

The time resolved fluorescence and anisotropy of subtilisins BPN′ and *Carlsberg*

J.M. Janot [c,*], A. Beeby [b], P.M. Bayley [a] and D. Phillips [b]

[a] *National Institute for Medical Research, Mill Hill, London, NW7 1AA (UK)*
[b] *Department of Chemistry, Imperial College, London SW7 2AY (UK)*
[c] *Laboratoire de Physico-Chimie des Systemes Polyphases, C.N.R.S route de Mende BP5051, 34033 Montpellier Cedex (France)*

(Received 20 November 1990; accepted in revised form 15 April 1991)

Abstract

Time-resolved emission and anisotropy have been measured for the tryptophan (Trp) residues of two closely related subtilisin proteins. The single Trp of subtilisin *Carlsberg* shows complex lifetime properties, and anisotropy consistent with a fast (ca. 200 ps) segmental motion, on the "wobbling in a cone model" the semi angle is in the range 38 to 47 degrees. The lifetime and anisotropy properties for this single Trp residue suggest that the predominant state is that of an effectively non-emitting statically quenched fluorophore. This fast component is also resolved in the anisotropy of subtilisin BPN′ but with relatively low amplitude, due to the dominant emission of the other Trp residues. The diversity of the photophysical properties is not readily correlated with the structure of the proteins, though the observed complexity is consistent with the likely heterogeneity of environment due to the surface location of all the Trp residues.

Keywords: Subtilisin; Fluorescence; Anisotropy; Lifetime; Photon-counting

1. Introduction

Time-resolved fluorescence measurements of intrinsic probes in proteins can be used to study dynamic and structural properties of proteins. Measurements of fluorescence anisotropy reveal the average angular displacement of the fluorophore during the lifetime of the emission. The accessibility of short time scales using picosecond pulsed lasers coupled with the high sensitivity of time-resolved fluorescence techniques gives information on internal motions of either tyrosine or tryptophan (Trp) residues in proteins, as well as global motions of whole proteins [1]. Assignment of fluorescence decay properties to individual residues in multi-tryptophan containing proteins is complex. Interpretation of such fluorescence is often complicated since multi-exponential decays are often observed even for single Trp proteins [1,2]. This behaviour of the Trp can be explained by characteristic properties of this indole chromophore molecule. Two transition dipoles (^1L_a and ^1L_b) are implicated in the near UV absorption region [3,4] and the stronger broad transition

* To whom correspondence should be addressed.

^1L_a almost completely overlays the second weaker ^1L_b transition [3–5]. At 300 nm the ^1L_a transition can be excited almost exclusively. Finally, energy transfer occurs efficiently between these transitions [6,7] and the observed fluorescence emission results partially from this process; the heterogeneous fluorescence lifetime observed at 345 nm (where only the ^1L_a transition is supposed to be involved) can be attributed to this mechanism [5]. In addition to the complex photophysics of the indole group, reorientation of (i) the solvent and (ii) chemical groups of the protein, near the excited fluorophore, can explain the multiplicity of observed lifetimes in proteins [8]. The existence of three different rotameric configuration of Trp is well established; the multiplicity of the ground states corresponding to these rotamers could also explain the multi-exponential decays [8–16].

In this report we present the time-resolved fluorescence and anisotropy of two homologous proteins; subtilisin BPN' and subtilisin *Carlsberg*, referred to as subtilisins B and C respectively. This pair of proteases have strong sequence homology and similar crystal structures; [17,18] they are approximately spherical with a diameter of ca. 42 Å [19]. Subtilisin B contains 275 amino acid residues, of which three are Trp and 10 tyrosine. The Trp residues at positions 106, 113 and 241, reside close to the exterior of the protein [19,20]. The single Trp residue of subtilisin C is at position 112, but due to a deletion in the sequence the homology is with subtilisin B's Trp-113: hence we refer to both as Trp-113. These proteins represent a pair of natural mutants which may be used to study the effects of residue substitution.

The fluorescence of the subtilisins has been shown to be complex [21–25]. Some confusion over the identity of the subtilisins used in previous work [22] has now been corrected [23]. The fluorescence from subtilisin C's Trp-113 is known to be strongly quenched and to exhibit complex decay kinetics. Willis and Szabo [24] have recently reported that the emission from subtilisin C excited at 295–305 nm has a contribution due to tyrosine residues, an unusual phenomenon for a protein containing Trp [25]. This emission was centered about 310 nm and was assigned a single fluorescence lifetime of 3.3 nm whereas the Trp emission covered the range 320–370 nm and had a bi-exponential decay. Subtilisin B is more fluorescent, although it was concluded that Trp-113 in this protein is also quenched and that the Trp fluorescence arises from Trp-106, (80%), and Trp-241, (20%) [26]. Willis and Szabo [24] reported complex 4-component decays from this protein.

The autolysis of the subtilisins is well known and protein fragments containing Trp, with fluorescence properties different from those of the parent protein, must be excluded. Treatment of subtilisin with phenyl methanesulphonyl fluoride, PMSF, is known to block the active site of the protease and therefore inhibit its autolysis. It may be argued that the protein is changed by this reaction therefore it is necessary to show that the properties of the protein, in particular its fluorescence, are not affected. Earlier UV-CD and steady state fluorescence measurements reported by Bayley et al. have indicated that for their subtilisin B or C, the secondary and tertiary protein structure and fluorescence of the native and inhibited proteins are identical [23]. Furthermore at appropriate protein concentrations, the materials were found to be stable for relative long periods. In the present work, in order to show that time-resolved fluorescence measurements are not affected by the formation of breakdown products, the fluorescence decays of both the inhibited and uninhibited proteins were measured. Previous measurements of the fluorescence anisotropy of subtilisin C [23] are extended and compared with those of subtilisin B. The aim was to see how far the characteristic fluorescence emission and anisotropy properties of Trp-113 in subtilisin C may be resolved from the more complex emission of the Trp residues of subtilisin B.

2. Experimental

Samples were obtained from the Sigma Chemical Company Ltd and purified by chromatography on a Superose-12 FPLC column in 0.1 *M* TRIS buffer at pH 7.5. Samples were assayed by UV-circular dichroism studies and by steady state

fluorescence. The purified protein fractions were immediately frozen and stored at −20 °C in TRIS buffer. Earlier studies [23] have demonstrated that samples prepared in this manner are stable. Inhibited samples, denoted BI and CI, were prepared by reaction of the native protein with PMSF and were purified by FPLC as described, [23].

2.1 Apparatus

The fluorescence decays were acquired by the technique of time correlated single photon counting [27]. The excitation source consisted of a synchronously pumped, cavity dumped rhodamine 6G dye laser, (Coherent 701 dye laser and 7220 cavity dumper) pumped by the output of a frequency doubled, mode locked Nd:YAG laser, (Coherent Antares 76-S), operating at a repetition rate of 76 MHz. The repetition rate of the dye laser was reduced to 3.8 MHz, giving a pulse width of less than 6ps and an average power of 150 mW at 590 nm. The vertically polarised output was rotated by 90 ° by a Fresnel double rhomb, (Spectra Physics 310-21) and then frequency doubled by an angle tuned KDP crystal (Lambda Physik FL31). Vertical polarisation of the UV radiation was ensured by passage through a Glan–Taylor prism, (excitation polariser).

The fluorescence was collected at 90 ° to the excitation and was detected by a Hamamatsu R1564U-01 microchannel plate detector, (MCP), after passage through an interference filter to select the desired emission wavelength, and a Glan–Taylor prism (emission polariser), rotated by a stepper motor. The output of the MCP was amplified by two LeCroy VT100B amplifiers in series and the pulses passed to an Ortec 584 constant fraction discriminator, providing the start pulse for the Ortec 547 time to amplitude converter; the stop being derived from the cavity dumper synchronous output after processing by an Ortec 454 timing filter amplifier. A histogram of detected photons was collected on a Canberra Series 30 multichannel analyser and subsequently transferred to an IBM-PC compatible for analysis. The instrument response function of the equipment was measured by the use of a dilute suspension of Ludox in water as a scattering solution and in the UV range was typically 70–100 ps FWHM. Decays of I_{ver} (decay of fluorescence recorded with the emission polariser set in the vertical position, i.e. parallel to the polarisation of the excitation) and I_{hor} (decay of fluorescence recorded with the emission polariser set in the horizontal position, i.e. perpendicular to the polarisation of the excitation) were recorded by repeated sequential acquisition of 20 or 40 seconds. The two traces were recorded into the two memory regions of the MCA (512 channels each) which was controlled by the microcomputer used to move the emission polariser's stepper motor. At the end of the acquisition the live times of the two decays were matched to account for the dead time of the MCA's pulse height analyser. The 'g' factor of the apparatus was determined by integration of I_{ver} and I_{hor} from a sample with a long lifetime and short rotational correlation time and was always found be unit. The efficiency of the emission polariser, estimated from the ratio of I_{hor}/I_{ver} for a scattering sample was found to be $< 1\%$. Contributions to the fluorescence from the 340, 360 and 380 nm interference filters were $< 0.01\%$ and from the buffer $< 0.2\%$. The fluorescence decays I_m were recorded with the emission polariser set to the magic angle (54.7 ° from the vertical position defined previously).

All fluorescence decays were acquired with a maximum count rate of 13 KHz, resulting in a counting efficiency of $< 0.3\%$. The time per channel was set in the range 10–40 ps/ch in order to (a) collect a well defined instrument response and (b) to improve the accuracy with which long decay components were measured. In order to verify that the system was performing well decays of 2,5-diphenyl oxazole in hexane, ($\tau_f = 1.25$ ns) were frequently measured at the magic angle as well as in the vertical and horizontal positions. *N*-acetyl tryptophanamide in water was also used as a reference material, $\tau_f = 2.95$ ns.

All the reported fluorescence decays at the magic angle were recorded to a minimum of 50,000 counts in the peak channel, having a typical total of 5×10^6 counts and for the anisotropy measurements typically 1×10^7 counts in total in both I_{ver} and I_{hor}.

2.2 Time-resolved fluorescence and anisotropy

2.2.1 Determination of the motion

The rotational motions of a Trp residue bound to a protein result from the superimposition of the motion of the residue in the protein and the global rotational motion of the protein. Many theories have been developed on this subject [7,28–31] in order to obtain an analytical expression of the time-dependent decay of anisotropy $r(t)$. Theoretically, for a completely assymetric body, this expression is expected to be the sum of five exponential decays [32]. The crystallographic structure of subtilisin BPN′ suggests that these proteins are effectively spherical [19]. In this case a single exponential decay is expected for the global motion. In practice the analysis of the decay of anisotropy can be performed using the expression [7,29]

$$r(t) = \left[r_{\mathrm{trp}}\, \mathrm{e}^{-t/\Phi_{\mathrm{trp}}} + r_{\mathrm{p}}\right] \mathrm{e}^{-t/\Phi_{\mathrm{p}}}$$

where Φ_{trp} is the correlation time for the motion of the fluorophore in the protein and Φ_{p} is the correlation time for the global motion of the protein. The parameter r_{p} is the residual anisotropy remaining after all faster motions have ceased.

In a model-dependent way the anisotropy r_{p} can be related to a semi-angle θ of a cone in which the chromophore transition dipole freely wobbles [30] using the relation:

$$r_{\mathrm{p}}/r(0) = \tfrac{1}{4}\{\cos\theta[1+\cos\theta]\}^2$$

where $r(0)$ is the anisotropy in the absence of motion; $r_{\mathrm{p}} + r_{\mathrm{trp}} = r(0)$, the initial anisotropy. It should be stressed that the above expression of $r(t)$ is only valid when either the absorption dipole or the emission dipole is parallel to the axis about when wobbling occurs. This assumption for a Trp is not clear, but a similar expression has been developed for such a case [7,29]. In the present paper we restrict our analysis to the simplest expression, accepting that the calculated values of θ are subject to this limitation.

The value of $r(0)$ depends on the angle between the absorption and emission dipoles. For the Trp residue the two transition dipoles $^1L_{\mathrm{a}}$ and $^1L_{\mathrm{b}}$ involved in the absorption process are nearly perpendicular and $r(0)$ is slightly different for both transitions [4]. The ratio of the absorption of the two transitions depends on the excitation wavelength; the observed values of the anisotropy $r(0)$ should therefore be different for an excitation at 295 and 300 nm. This effect has been observed for number of single Trp peptides and proteins [32].

2.2.2 Data analysis

In order to extract lifetimes and correlation times from the experimental decays a program using the Marquardt algorithm [33] has been used. Assuming a linear response of the apparatus, the experimental decay curves $F(t)$ were fitted by convolution [34] of a calculated fluorescence decay $f(t)$ with the excitation pump profile $P(t)$ obtained from a scattering sample. The fluorescence decay law $s(t)$ and the anisotropy decay law $r(t)$ were related to the emission by the relations.

$$i_{\mathrm{ver}}(t) = \tfrac{1}{3}s(t)[1+2r(t)],$$

$$i_{\mathrm{hor}}(t) = \tfrac{1}{3}s(t)[1-r(t)]$$

or

$$s(t) = i_{\mathrm{ver}}(t) + 2i_{\mathrm{hor}}(t),$$

$$r(t) = \frac{i_{\mathrm{ver}}(t) - i_{\mathrm{hor}}(t)}{i_{\mathrm{ver}}(t) + 2i_{\mathrm{hor}}(t)}$$

and the corresponding experimental decays (where * indicates convolution)

$$I_{\mathrm{ver}}(t) = P(t) * \{\tfrac{1}{3}s(t)[1+2r(t)]\},$$

$$I_{\mathrm{hor}}(t) = P(t) * \{\tfrac{1}{3}s(t)[1-r(t)]\}$$

$$I_{\mathrm{m}}(t) = I_{\mathrm{ver}}(t) + 2gI_{\mathrm{hor}}(t)$$

where g is the correction factor that accounts for polarisation dependence of the optics. The experimental decays $s(t)$ and the anisotropy $r(t)$ were analysed as sums of exponential:

$$s(t) = \sum a_i\, \mathrm{e}^{-t/\tau_i} \quad \text{and} \quad r(t) = \sum b_j\, \mathrm{e}^{-t/\Phi_j}$$

where τ_i is the fluorescence lifetime, a_i the contribution to the total fluorescence of emission i; and the apparent correlation times Φ_j and ampli-

tudes b_j related to the model used for the anisotropy (cf. Section 2.2.1.). For $j = 2$, the constants Φ_1 and Φ_2 can be related to the parameters Φ_{trp} and Φ_p of the "wobbling in the cone" model by $\Phi_2 = \Phi_p$ and $1/\Phi_1 = 1/\Phi_p + 1/\Phi_{trp}$.

In our program the lifetimes were estimated either from the decay curves collected at the magic angle (54.7°), $I_m(t)$, or from the corresponding calculated sum curve defined as: $I_{ver}(t) + 2gI_{hor}(t)$.

The anisotropy decay curves were analysed directly from the expressions of I_{ver} and I_{hor}, using the values τ_i and a_i obtained from the sum curve and the parameters Φ_j and b_j optimized by the simultaneous fit of both decays I_{ver} and I_{hor}.

A Poissonian distribution of counts has been assumed in the calculation of the reduced χ^2 defined as:

$$\chi^2 = \frac{1}{n_2 - n_1 + 1 - p} \sum_{i=n_1}^{n_2} \frac{[I(t_i) - Y(t_i)]^2}{\mathrm{var}[I(t_i)]}$$

where n_1 and n_2 are the first and the last channels of the decay $I(t_i)$, p the number of fitting parameters and $Y(t)$ the decay calculated as the convolution of the pump profile with the exponential decay of parameters τ_i and a_i. The theoretical value of χ^2 for a good fit is defined as equal to 1.0.

The analysis was performed from the maximum of the decays in order to avoid the problem in the convolution of the leading edge of the decay. This problem is found very often in the photon counting technique and is not clearly understood. It seems to increase as the time resolution is increased by the use of excitation pulses of very short time duration. We performed simulations of multi-exponential decays, including a very fast component; the analysis from the maximum of these decays gave the consistent results, confirming the validity of this approach.

The weighting factors were calculated as [35]:

$$\mathrm{var}[I(t)] = \sqrt{I(t)}$$

with $I(t)$ accounting for $I_m(t)$, I_{ver} and I_{hor}

$$\mathrm{var}[I_{ver}(t) + 2gI_{hor}(t)] = \mathrm{var}[I_{ver}(t)] + 4g^2\ \mathrm{var}[I_{hor}(t)]$$

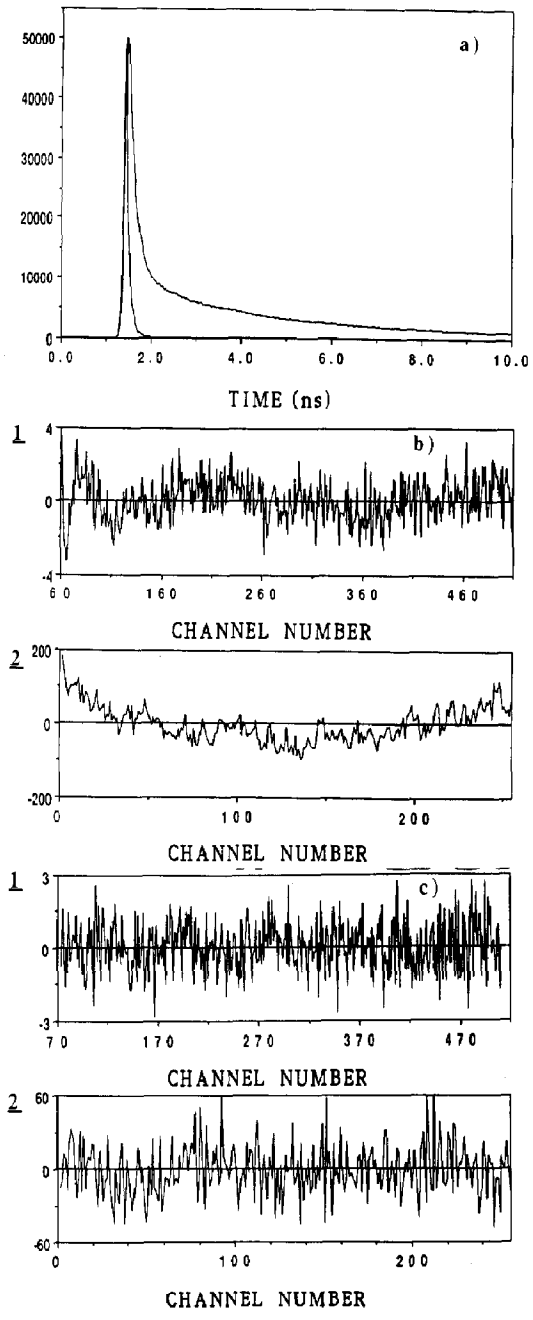

Fig. 1. (a) Decay of fluorescence of subtilisin *Carlsberg* recorded at 360 nm under excitation at 295 nm. (b) 1 Weighted residual and 2 autocorrelation function of the weighted residual for a three exponential fit. (c) 1 Weighted residual and 2 autocorrelation function of the weighted residual for a four exponential fit.

Table 1a

Fluorescence lifetime analysis of subtilisin C and the inhibited protein CI. (Lifetimes are in ns, Yields, Y, are the percentage contribution of the component to the total emission; $Y_i = a_i\tau_i / \sum_j a_j\tau_j$. λ_{em} are in nm. χ^2 as defined in the text)

λ_{em}	τ_1	Y_1	τ_2	Y_2	τ_3	Y_3	τ_4	Y_4	χ^2
Subtilisin C, Excitation 295 nm									
340	0.065	8	0.185	11	1.464	19	4.644	61	1.11
360	0.082	8	0.217	8	1.439	20	4.722	64	1.06
380	0.089	7	0.252	6	1.464	20	4.820	68	1.09
Subtilisin CI, Excitation 295 nm									
340	0.094	8	0.170	13	1.328	16	4.597	63	1.14
360	0.059	6	0.201	9	1.399	19	4.962	66	1.17
380	0.083	6	0.246	6	1.447	17	5.105	70	0.99
Subtilisin C, Excitation 300 nm									
340	0.041	6	0.148	9	1.343	11	4.908	74	1.10
360	0.088	6	0.278	6	1.589	18	5.307	70	0.98
380	0.070	4	0.220	5	1.360	15	5.012	76	1.15
Subtilisin CI, Excitation 300 nm									
340	0.046	9	0.175	11	1.478	16	5.063	64	1.04
360	0.097	8	0.287	6	1.517	16	5.402	70	1.27
380	Not measured								

The number of exponentials used for the fit was increased until a satisfactory fit was obtained (random distribution of the residuals) for a minimum of χ^2. Other statistical parameters were used routinely in order to judge the result of the analysis: the Durbin–Watson parameter [36,37], the skewness factor, the kurtosis factor [27,38] as well as the autocorrelation function of the residuals.

In order to test the possibility to improve the fit further, the shift that experimentally occurs between the pump profile and the decay was also introduced as a fitting parameter. The shifted pump shape was calculated by a linear interpolation method. This parameter was never found to be higher than one and a half channels.

The analysis of I_{ver} and I_{hor} was performed simultaneously on both decays. The global reduced χ^2 was calculated as the mean value of the reduced χ^2 obtained for both decays.

Table 1b

Fluorescence lifetime analysis of subtilisin B and the inhibited protein BI (symbols as defined in Table 1a)

λ_{em}	τ_1	Y_1	τ_2	Y_2	τ_3	Y_3	χ^2
Subtilisin B, Excitation 295 nm							
340	0.224	4	1.605	11	7.016	85	1.06
360	0.273	2	1.759	9	7.082	89	1.08
380	0.295	3	1.760	13	6.960	85	1.27
Subtilisin BI, Excitation 295 nm							
340	0.208	4	1.503	10	6.945	86	1.24
360	0.220	2	1.554	8	7.007	90	1.18
380	0.266	2	1.628	9	7.003	89	1.07
Subtilisin B, Excitation 300 nm							
340	0.199	3	1.408	10	7.013	87	1.08
360	0.291	2	1.669	9	7.007	89	1.17
380	0.328	2	1.645	11	6.942	87	1.01

3. Results and Discussion

Figures 1(a) and 1(b) show the quality of fit obtained from analysis of the fluorescence decays of subtilisin C using either three or four components, respectively. The improved χ^2 and the autocorrelation function (and other statistical criteria) indicate the significance of including a short (fourth) component. In other experiments with single short-lived fluorophores and with calmodulin (unpublished), no such component was detected. It therefore appears to be a true component of the emission from this protein, and not an experimental artifact. The full numerical analysis of fluorescence emission of subtilisin C (Table 1a) shows multiple components for all combinations of excitation and emission wavelengths. Similar properties are found for both the natural and PMSF-inhibited enzyme. Best fits were consistently found using a four exponential analysis; 148–287 ps (yield 5–13%), 1.3–1.6 ns (yield 11–20%), 4.6–5.5 ns (yield 61–76%), including the minor component (yield 5-10%) with lifetime 60–90 ps. The lifetimes appear to increase slightly with increasing emission wavelength. There is a general trend of an increasing lifetimes with increasing emission wavelength; this behavior has been observed in many different proteins [9,10,39–41], and has been explained either by the presence of multiple ground states with different emission spectra [9] such that the red-shifted components have the longer lifetimes, or by the effect of the relaxation of the solvent or of polar moieties of the protein about the chromophore [42].

The analysis for excitation at 300 nm and 295 nm show similar patterns. The contribution to the total emission for each component at both excitation wavelengths are nearly identical at each emission wavelength suggesting a similar emission spectrum for all these components at both excitation wavelengths. We therefore find no evidences to associate any of these components with Tyr emission, as expected for this range of Trp emission wavelengths. The complexity of the lifetime behaviour is noteworthy; the emission is highly quenched, and it appears possible that multiple conformations and the heterogeneous environment of the fluorophore may contribute to this effect (Examination of the crystal structure, using the molecular graphics package FRODO this residue appears to be in a solvent-exposed pocket).

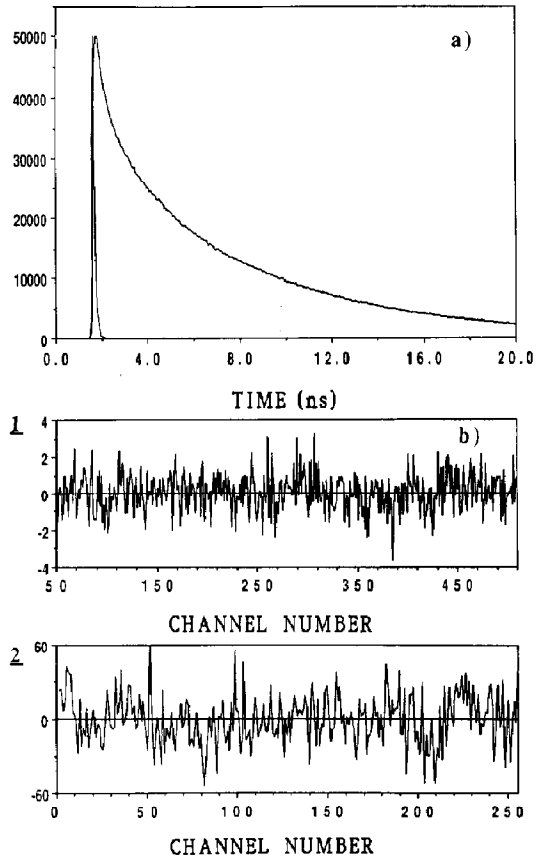

Fig. 2. (a) Decay of fluorescence of subtilisin BPN' recorded at 360 nm under excitation at 295 nm with the corresponding (b) 1 weighted residual and 2 autocorrelation function of the weighted residual for a three exponential fit.

By contrast, the much stronger emission of subtilisin B (Table 1b) shows a consistent pattern of three-exponential decays. The quality of fit is shown in Fig. 2. The predominant component (yield 80–90%) has a lifetime of 6.9 to 7.1 ns with the shortest component (yield 2 to 4%) decaying with a $\tau \approx 200$ to 300 ps. Similar patterns are found for natural and PMSF-inhibited enzyme, and for all wavelength combinations used. For this protein, with three Trp residues per molecule, it is clearly impossible to assign lifetime compo-

nents to individual residues, and in any case, the example of subtilisin C shows that the emission from Trp-113 (which is nearly non-fluorescent in this protein [26]), is itself highly complex. The longest lifetime accounts for 85–90% of total emission in all cases; trends with emission wavelength are less pronounced than with Subtilisin C, although there is again an overall tendency for the lifetimes to increase with emission wavelengths.

The lifetime results may be compared with data from Willis and Szabo [24]. Firstly, as shown in a previous report, the purified subtilisins used here show little or no signs of degradation from autolysis during the course of fluorescence experiments [23]. Lifetime data were effectively reproducible for these low concentration samples kept at 20 °C for periods of up to 6 hours. The data presented here are in broad agreement with the more limited data presented previously, but differ from the results of Willis and Szabo [24] in certain details. We found that four component fits were necessary for subtilisin C compared with the 3 component fit for B, whereas Willis and Szabo [24] found the reverse. Analysis of the fluorescence of subtilisin B using a four exponential model introduced an additional short component with a $\tau \approx 60$ ps as in [24], but there was no significant improvement in the fit. The calculated emission spectra presented in [24] show only a weak contribution of this short component at the wavelengths used. Thus, although we cannot reject the possibility of an additional 60 ps emission in this protein, we find no reason to include it.

Willis and Szabo [24] report the major lifetime for subtilisin B as 8.0 ns which they assigned to the emission of an exposed Trp. This long component is similar to the 6.9–7.1 ns component we observed; the discrepancy between these values is may be related to the fact that we analyse with only three lifetimes (instead of four) and also to the different extents of the time ranges used.

The calculated time-resolved anisotropy of subtilisin C, generated from the observed parallel and perpendicular decays is show in Fig. 3. Inspection of this curve shows the process to be complex, indicating multiple motions of the fluorophore. Analysis was made of the observed orthogonally polarised components of the fluorescence emission on a model allowing segmental and global motions, and coupling of these to all lifetime components [6]. Table 2(a) shows that there is a significant fast component 150–300 ps with a longer component of 13–17 ns that agrees with the theoretical value of approximately 12 ns for the global rotation of a hydrated spherical protein of M_r 30 kDa in aqueous solution at 25 °C [43].

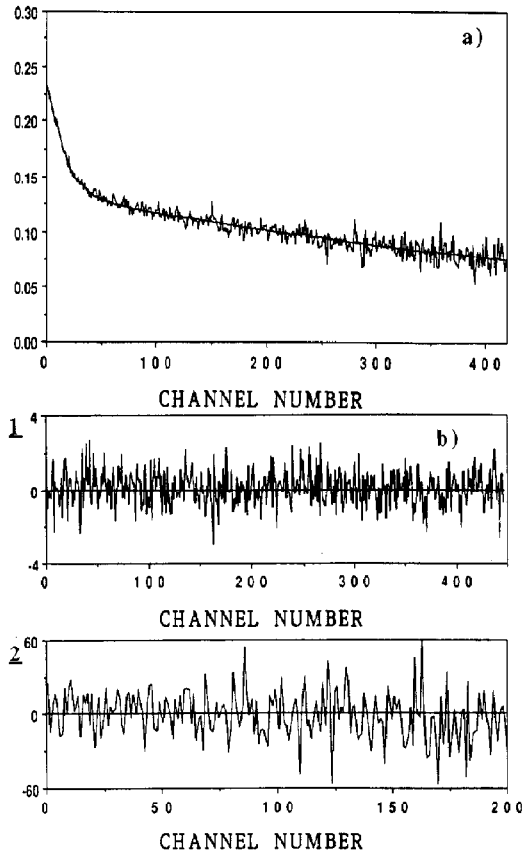

Fig. 3. (a) Decay of anisotropy of fluorescence of subtilisin *Carlsberg* calculated from the experimental fluorescence decays I_{ver} and I_{hor}. The fitted decay of anisotropy $r(t)$ has been calculated using the parameters (Φ_i and r_i) obtained from the fits of I_{ver} and I_{hor}. (b) 1 Weighted residual, 2 autocorrelation function of the weighted residual. The time per channel was set to 20 ps/ch in this experiment. The weighted residual has been calculated using as weighting factor the expression [35]: $\mathrm{var}[r(t)] = 9I_{ver}(t)\cdot I_{hor}(t)\cdot[I_{ver}(t)+I_{hor}(t)]/(I_{ver}(t)+2I_{hor}(t))^4$.

Table 2a

Fluorescence anisotropy analysis of subtilisin C and the inhibited protein CI (χ^2 is the fitting criterion for the analysis of I_{ver} and I_{hor} as described in the text). Rotational correlation times (lifetimes are in ns)

λ_{em}	ϕ_{trp}	r_{trp}	ϕ_p	r_p	r_o	θ	χ^2
Subtilisin C, Excitation 295 nm							
340	0.300	0.128	16.82	0.084	0.212	47	1.01
360	0.278	0.156	16.10	0.101	0.257	44	1.01
380	0.257	0.118	17.45	0.075	0.193	49	1.12
Subtilisin C, Excitation 300 nm							
340	0.148	0.211	13.13	0.178	0.389	33	1.14
360	0.221	0.118	16.78	0.173	0.291	34	0.98
380	0.149	0.173	14.00	0.100	0.273	46	1.14

The corresponding calculated time-resolved anisotropy of subtilisin B is shown typically in Fig. 4. With a similar analysis of the polarised emission components, we resolved a fast motion of 140 to 240 ps, and a longer correlation time of about 14 ns, very close to the value found for subtilisin C, as expected from their high homology [19]. In this case, the fast component appears with smaller amplitude, consistent with this being derived from an individual Trp residue, likely, by analogy with the anisotropy decay of subtilisin C to be Trp-113. This interpretation has to be made with care, since the model of analysis used for the anisotropy assumes that all lifetimes are associated with all correlated times. Nevertheless the analysis using uncoupled models shows similar results (not shown) so long as the model is restricted to a combination of three lifetimes and two correlation times. Similar analysis of the anisotropy of subtilisin B has been performed

Table 2b

Fluorescence anisotropy analysis of subtilisin B and the inhibited protein BI. Rotational correlation times (lifetimes in ns)

λ_{em}	ϕ_1	r_1	ϕ_2	r_2	r_o	χ^2
Subtilisin B, Excitation 295 nm						
340	0.215	0.045	14.89	0.194	0.239	1.35
360	0.238	0.042	14.30	0.162	0.204	1.15
380	0.162	0.065	14.57	0.157	0.222	1.17
Subtilisin B, Excitation 300 nm						
340	0.234	0.038	13.76	0.265	0.303	1.16
360	0.141	0.048	15.25	0.242	0.290	1.16
380	Not measured					

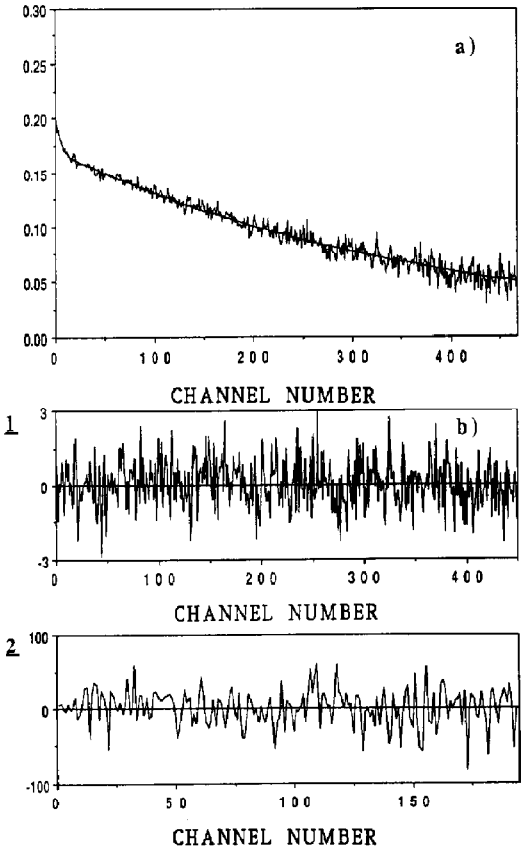

Fig. 4. (a) Decay of anisotropy of fluorescence of subtilisin BPN' calculated from the experimental fluorescence decays I_{ver} and I_{hor}. (b) 1 Weighted residual, 2 autocorrelation function of the weighted residual. The time per channel was set to 40 ps/ch in this experiment. See legends of Fig. 3.

using a four exponential fit for the fluorescence decay; similar results were found for the correlation time.

The average values of $r(0)$ for subtilisin C calculated as the sum of r_{trp} and r_p in Table 2(a) over all the emission wavelengths are equal to 0.221 and 0.318 for excitation 295 nm and 300 nm, respectively. These values may be compared with the average value obtained for static measurements of a number of single Trp peptides and proteins reported in [32], 0.177 (excitation 295 nm) and 0.263 (excitation 300 nm), but also with 0.250 (295 nm) reported for Trp in [4]. These measurements are in cryosolvents at $-58\,^{\circ}$C. The reason for the discrepancy between our result and [32] could be due to a different solvent-de-

pendent shift of the absorption spectrum. The magnitude of the $r(0)$ values calculated suggests that we are not missing faster depolarisation processes, as expected from the time resolution of our system (a tenth of the detected FWHM of the pump profile ≈ 7–9 ps). As mentioned previously, the emission of fluorescence and consequently the anisotropy at a given excitation wavelength results from contributions of ^1L_a and ^1L_b excited states. Since the anisotropy $r(0)$ for the transitions ^1L_a and ^1L_b are different ($r(0)_a$: 0.33, $r(0)_b$: -0.165 for Trp in propylene glycol at $-58\,^\circ$C (4]) a change of the observed $r(0)$ with excitation wavelength, is not surprising. The decrease of $r(0)$ could reflect a higher relative contribution of the ^1L_b transition at shorter excitation wavelength. Using $r(0)$: 0.260 and $r(0)$: 0.3 (average values calculated from all our data) for excitation 295 nm and 300 nm the calculated semi-angles θ in the cone model (cf. Materials and Methods [30]) are $47 \pm 2\,^\circ$ and $38 \pm 6\,^\circ$ respectively for subtilisin C.

The values of (i) the correlation time associated with the internal motion and (ii) the semiangle of the cone associated with wobbling of the chromophore, suggest that Trp-113 must be relatively free to execute independent motion and is therefore not buried in the protein. These deductions must be weighed against the high degree of quenching shown by this Trp residue. The lifetime data shows that the emission, although very low in total quantum yield, still contains components (up to several ns) characteristic of normal Trp emission. This behavior is characteristic of static quenching (as opposed to dynamic or collisional quenching). It would therefore, be consistent with all the fluorescence emission data that Trp-113 is involved in a complex of mean lifetime much greater than the nano-second time scale of fluorescence, and this complex is effectively non-emitting. The observed emission, which is highly depolarised, appear therefore to derive from Trp-113 in the small fraction of time in which it is free to move over a relatively wide cone semi-angle.

The average values of $r(0)$ for subtilisin B calculated as the sum of r_1 and r_2 in Table 2(b) over all the emission wavelengths are equal to 0.227 and 0.295 for excitation 295 nm and 300 nm respectively. From these values we deduce that we are not missing faster depolarisation processes. From the values of r_2 we can conclude that most of the fluorescence emission is depolarised in the time course of the global motion of the protein. As mentioned before the major component of emission in this protein has a lifetime 6.9–7.1 ns and can be assigned to the emission of an exposed Trp [24]. From these results, it seems that most of the emission of fluorescence of Subtilisin B originates from exposed Trp residues wich experience mainly the global Brownian rotation of the whole protein. It is tempting to assign the fast depolarisation process to the Trp-113 of subtilisin B by comparison of the results obtained for the subtilisin C. The calculation of θ has not been performed in this case.

These results have bearing on the ability of time-resolved fluorescence to provide information on the conformation and dynamics of multiple-Trp containing proteins, and the possibility of using mutant proteins, either natural, as used here, or those derived by protein engineering techniques, to provide detailed structural information about a given protein. The initial intention was to compare the properties of the single Trp protein, subtilisin C, with the comparable residue in the three Trp protein, subtilisin B. In fact this proves unusually difficult in the case of subtilisin, since the emission from Trp-113 in subtilisin C is very heavily quenched, and its photophysical properties are extremely complex. In subtilisin B, by comparison, the much stronger total Trp emission contains contributions from Trp-106 and Trp-241, and apparently these dominate the derived lifetime parameters. In anisotropy, however, fast (presumed segmental) motion is shown by Trp-113 in subtilisin C, and there is evidence for such motion in the anisotropy properties of Subtilisin B. Clearly a more detailed resolution would be possible using derivatives of subtilisin B from which Trp residues have been selectively substituted with other residues. Finally, it is pertinent to note that the subtilisins are unusually stable proteins, with little evidence from other sources about large scale internal motions. It seems reasonable to conclude therefore that the mobile Trp residue provides dy-

namic information only about a very localised region of the overall structure.

Acknowledgements

The authors would like to express their thanks to Dr. Garry Rumbles for assistance with the laser system, Dr. Ian Tickel for access to the FRODO molecular graphics program, Dr. Ismaël Moya for advice in mathematical analysis and to SERC for financial support under grant number GR/D/79821. Dr. Jean-Marc Janot was supported by a Fellowship under the E.C. Science Plan (Twinning Grant) Number: 852-00255 UK: 05 PUJU1.

References

1 J.M. Beechem and L. Brand, Annu. Rev. Biochem. 54 (1985) 43–71.
2 R.B. Cundall and R.E. Dale, Time-resolved fluorescence spectroscopy in biochemistry and biology (Plenum Press, New York, NY, 1983).
3 Y. Yamamoto and J. Tanaka, Bull. Chem. Soc. Jpn. 45 (1972) 1362.
4 B. Valeur and G. Weber, Photochem. Photobiol. 25 (1977) 441.
5 S.V. Konev, in: Fluorescence and phosphorescence of proteins and nucleic acids, ed. S. Udenfriend (Plenum Press, New York, NY, 1967), chap. 1.
6 A.J. Ross, D.H. Waldeck and G.R. Fleming, J. Chem. Phys. 78 (1983) 6455–6467.
7 A. Szabo, J. Chem. Phys. 81 (1984) 150–167.
8 J.B.A. Ross, K.W. Rousslang and L. Brand, Biochemistry 20 (1981) 4361.
9 A.G. Szabo and D.M. Rayner, J. Am. Chem. Soc. 102 (1980) 554.
10 S.A. Cockle and A.G. Szabo, Photochem. Photobiol. 34 (1981) 23.
11 A. Grinvald and I.Z. Steinberg, Biochim. Biophys. Acta 427 (1976) 663.
12 G. Hazan, E. Haas and I.Z. Steinberg, Biochim. Biophys. Acta 434 (1976) 144.
13 A.G. Szabo, T.M. Stepanik and D.M. Wayner, Can. J. Biochem. 58 (1980) 898.
14 J.W. Petrich, M.C. Chang, D.B. McDonald and G.R. Fleming, J. Am. Chem. Soc. 105 (1983) 3824.
15 E. Gudgin, R. Lopez-Delgado and W.R. Ware, Can. J. Chem. 59 (1981) 1037.
16 R.D. Ludescher, J.J. Volwerk, G.H. de Haas and S.B. Hudson, Biochemistry 24 (25) (1985) 7240–7259.
17 C.A. McPhalen, H.P. Schnebli and N.M. James, FEBS Lett. 88 (1985) 55–58.
18 W. Bode, E. Papamokos, D. Musil, U. Seemueller and H. Fritz, EMBO. J. 5 (1986) 81.
19 C. Schubert, R. Wright, A. Alden and J. Kraut, Nature 221 (1969) 235.
20 E.L. Smith, F.S. Markland, C.B. Kasper, R.J. Delange, M. Landon and W.H. Evans, J. Biol. Chem. 241 (1966) 5974–5976.
21 P.M. Bayley, Biophys. J. 49 (1986) 105a.
22 P.M. Bayley, S.R. Martin and R.W. Wijnaendts van Rensandt, in: Structure, dynamics and function of biomolecules, eds. A. Ehrenberg, R. Rigler, A. Gräslund and L. Nilsson, Springer-Series in Biophysics, Vol. 1 Springer, Heidelberg, 1987) pp 159–164.
23 P.M. Bayley, J.M. Janot and S.R. Martin, FEBS Lett. 250 (1989) 389–394.
24 K.J. Willis and A. Szabo, Biochemistry 28 (1989) 4902.
25 J.W. Longworth in: Time-resolved fluorescence spectroscopy in biochemistry and biology, eds. R.B. Cundall and R.E. Dale (Plenum Press, New York, NY, 1983) pp. 651–725.
26 M. Shopova and N. Genov, Int. J. Peptide Protein Res. 21 (1983) 475–478.
27 D.V. O'Connor and D. Phillips, Time correlated single photon counting (Academic Press, New York, NY, 1984).
28 D. Wallach, J. Chem. Phys. 47 (1967) 5258–5268.
29 G. Lipari and A. Szabo, Biophys. J. 30 (1980) 489–506.
30 K.Jr. Kinosita, S. Kawato and A. Ikegami, Biophys. J. 20 (1977) 289–305.
31 Y. Gottlieb and P. Walh, J. Chim. Phys. Phys. Chim. Biol. 60 (1963) 849–856.
32 J.R. Lakowicz, B.P. Maliwal, H. Cherek, H. and A. Balter, Biochemistry 22 (8) (1983) 1741–1752.
33 D.W. Marquardt, J. Soc. Ind. Appl. Math., 11 (1963) 431.
34 A. Grinvald and I.Z. Steinberg, Anal. Biochem. 54 (1974) 583.
35 R.E. Dale, in: Time-resolved fluorescence spectroscopy in biochemistry and biology, edn. R.B. Cundall and R.E. Dale (Plenum Press, New York, NY, 1983) pp. 555–604.
36 J. Durbin and G.S. Watson, Biometrika 37 (1950) 409.
37 J. Durbin and G.S. Watson, Biometrika 38 (1951) 159. A. Grinvald, Anal. Biochem., 75 (1976) 260.
38 R.A. Lampert, L.A. Chewter and D. Phillips, Anal. Chem. 55 (1983) 68–73; J.B. Birks, (Wiley-Interscience, New York, NY, 1970).
39 J.C. Brochon, P. Wahl, M. Charlier, J.C. Maurizot and C. Helene, Biochem. Biophys. Res. Commun. 79 (1977) 1261.
40 J.B.A. Ross, C.J. Schmidt and L. Brand, Biochemistry 20 (1981) 4369.
41 J.P. Privat, P. Wahl and J.C. Auchet, Biophys. Chem. 11 (1980) 239.
42 J.R. Lakowicz, Principles of fluorescence spectroscopy (Plenum Press, New York, NY, 1983).
43 C.R. Cantor and P.R. Schimmel, in: Biophysical chemistry, Part II (W.H. Freeman and Co, San Francisco, CA, 1980) p. 460.